THE ASTRONOMICAL JOURNAL, 123:142–158, 2002 January

SPECTROSCOPY OF GALAXIES IN THE BOOTES VOID

SHAWN CRUZEN AND TARA WEHR
Mead Observatory, Department of Chemistry and Geology, Columbus State University, Columbus, GA 31901; scruzen@ccssc.org, tara@ccssc.org

DONNA WEISTROP
Department of Physics, University of Nevada at Las Vegas, Las Vegas, NV 89154; weistrop@nevada.edu

RONALD J. ANGIONE
Department of Astronomy, San Diego State University, San Diego, CA 92182; angione@mintaka.sdsu.edu

AND

CHARLES HOOPES
Department of Physics and Astronomy, Johns Hopkins University, Baltimore, MD 21218; choopes@pha.jhu.edu
Received 2001 August 19; accepted 2001 October 4

ABSTRACT

We investigate the physical properties of a sample of 26 galaxies in the Bootes void and classify these galaxies based on the emission lines in their spectra. Fourteen galaxies are classified as H II galaxies with properties similar to field H II galaxies. Two of these galaxies, 1432+5302 and 1507+4554, are extreme starburst galaxies. Approximately half of the galaxies with measurable Hα + [N II] emission have elevated rates of star formation. Analysis of the galaxy continua suggests that approximately one-third of the void galaxies have large populations of blue stars. Stellar absorption features from metals in more than half the galaxies in the sample indicate the presence of late-type stars. Emission lines are detected from the H I galaxy 1517+3949 for the first time. Two systems, 1510+4727 and 1517+3956, are identified as closely interacting galaxy pairs, bringing the total number of known galaxy pairs in the void to four. The galaxy 1458+4944 is a LINER, making at least five AGNs in the void. Classifications of eight galaxies in the sample remain unknown. The galaxies in the Bootes void are similar to field emission-line galaxies with respect to stellar populations, emission-line properties, fraction of AGN and fraction of galaxy pairs. This result is inconsistent with some models of galaxy formation in low-density environments.

Key words: galaxies: evolution — galaxies: formation — galaxies: starburst — large-scale structure of universe

1. INTRODUCTION

Understanding the role that environment plays in the process of galaxy formation and evolution is one of the most important problems in astrophysics. Observations of the physical characteristics of galaxies in various environments have led to morphology-density relations such as those proposed by Dressler (1980), Postman & Geller (1984), and Giovanelli, Haynes, & Chincarini (1986). These studies have shown that the fraction of galaxies with different morphological types varies over several orders of magnitude with the galaxy space density. In general, the relative numbers of S0 and elliptical galaxies increase with space density, while the fractions of spiral and irregular galaxies decrease. Although much of the work in this area has emphasized cluster populations, the environmental influence on the formation of galaxies in low-density regions must also be understood for the model to be comprehensive. Investigations into the properties of galaxies in low-density regions will provide useful information on the role of environment in galaxy formation and evolution.

Analysis of the spatial distribution of galaxies in redshift surveys has shown the existence of large regions where the space density of galaxies is low (de Lapparent, Geller, & Huchra 1986; Vogeley, Geller, & Huchra 1991; da Costa et al. 1994; El-Ad & Piran 2000; Müller et al. 2000). These regions appear to be characteristic of the large-scale structure of the universe and to be arranged in a hierarchical system of voids and supervoids (Lindner et al. 1995). A reconstruction of the nearby matter density field by da Costa et al. (1996), in which the peculiar velocities of late-type spirals were derived from the Tully-Fisher relation, has shown that these deficiencies in the distribution of galaxies delineate real voids in the underlying distribution of matter and that these voids are more abundant than previous work had shown.

The Bootes void was first identified by Kirshner et al. (1981) and is centered at right ascension = 14^h50^m, decl. = +46°, v = 15,500 km s^{-1}, with a redshift range of $z = 0.041$ to $z = 0.062$ corresponding to a spherical region of radius 42 Mpc (H_0 = 75 km s^{-1} Mpc^{-1}). At the time of the void's discovery, only two emission-line galaxies (ELGs), I Zw 81 and Mrk 845, were known within this region. From a pencil-beam survey, Kirshner et al. (1987) estimated that there was only a 1% chance that the density of normal galaxies in the void is higher than 25% of the cosmic mean density.

Currently, the known Bootes void population includes ELGs, unevolved galaxies detected in H I emission, and galaxies with strong infrared emission detected by the *Infrared Astronomical Satellite* (*IRAS*) (Table 1). The number density of bright ELGs in the Bootes void has been estimated to be about $\frac{1}{3}$ that of the field distribution of bright ELGs (Weistrop 1989). The number density of *IRAS* galaxies in the void is between $\frac{1}{3}$ and $\frac{1}{6}$ that of the normal density of *IRAS* galaxies having the highest flux quality at 60 μm (Dey, Strauss, & Huchra 1990). The number density of galaxies in the void with significant X-ray emission is also

TABLE 1
GALAXIES IN OUR BOOTES VOID SAMPLE

Galaxy (1)	ID (2)	Published z (3)	Reference (4)
1345+4641	...	0.052	1
1357+4641[a]	...	0.054	1
1406+4905[b]	I Zw 81	0.05156	2
1407+4840[b]	CG 910	0.04336	3
1408+4852	CG 370	0.0444	4
1413+5056[b]	...	0.04922	5
1428+5255[a,b]	...	0.04448	3
1432+5302	CG 474	0.0446	6
1444+4402[b]	CG 538	0.04324	5
1446+4457[a]	CG 547	0.0432	7
1457+4228	CG 598	0.05743	8
1458+4944[a]	CG 922	0.0475	9
1503+5428	CG 620	0.0478	9
1505+3958	CG 629	0.0518	4
1506+5138[a]	Mrk 845	0.04542	7
1507+4554	CG 642	0.04837	7
1510+4727	CG 657	0.0527	7
1517+3949	...	0.0474	10
1517+3956[b]	CG 684	0.04701	8
1519+5050[a,b]	CG 692	0.0566	5
1530+4332A[b] ...	Main	0.05164	5
1530+4332B[b] ...	Companion	0.05164	5
1535+3831[b]	...	0.05078	5
1537+5315[b]	...	0.05196	5
1540+5013[b]	...	0.05427	5
1547+5121[b]	...	0.04985	3

[a] *IRAS* galaxy.
[b] X-ray source (Kim et al. 2001).

REFERENCES.— (1) Schneider et al. 1994; (2) Sargent 1970; (3) Strauss & Huchra 1988; (4) Weistrop 1989; (5) Dey et al. 1990; (6) Weistrop & Downes 1988; (7) Moody et al. 1987; (8) Tifft et al. 1986; (9) Lipovetsky see Weistrop et al. 1995; (10) Szomoru et al. 1993.

found to be about $\frac{1}{3}$ that of the field density (Kim et. al. 2001).

Previously, we obtained photometric imaging of a sample of galaxies in the Bootes void in broadband *BVRI* filters. From these data, the magnitudes and colors of the galaxies were determined and the morphological properties were examined. The results of this imaging survey (Cruzen, Weistrop, & Hoopes 1997, hereafter C97) showed that the Bootes void galaxies tend to (1) be brighter than field ELGs at similar redshift, (2) have blue broadband colors suggesting young stellar populations, and (3) contain a large fraction (>40%) of morphologically disturbed systems. These findings are consistent with other recent work on galaxies in low-density environments, although varying selection effects between samples must be carefully considered. Grogin & Geller (1999, 2000) report that galaxies in the lowest-density environments (less than half the mean field density) in the Center for Astrophysics Redshift survey (CfA2) have bluer broadband colors, show larger values for the EW(Hα) implying active star formation, and tend more toward late-type, irregular, or peculiar morphologies than do similar galaxies at densities up to twice the mean field density. The morphological similarities between the sample of C97 and that of Grogin & Geller (a magnitude-limited sample) are noteworthy because the Bootes void also constitutes a region where the galaxy density is less than half the mean field density. Surveys of galaxies in nearby voids ($z \leq 0.033$) selected based on the flux of emission lines indicate that these void ELGs are blue compact dwarfs, and have luminosities, colors, and star formation rates similar to their field counterparts (Popescu, Hopp, & Rosa 1999; Vennik, Hopp, & Popescu 2000). Imaging of our void sample, likewise selected partially on the basis of emission lines, also indicates color and morphological characteristics similar to field ELGs (C97), but absolute magnitudes that would exclude most from being classified as dwarfs by the criterion ($M_B < -18.5$) used by Popescu et al. (1999).

To follow up the imaging results, we have conducted a long-slit spectroscopic survey of our sample. The goal is to analyze the spectroscopic data to better understand the physical properties of the galaxies, as well as the energetic processes taking place within them. Peimbert & Torres-Peimbert (1992, hereafter PTP) have presented spectrophotometry for 10 of these galaxies. However, spectra for most of our sample have not been published, nor have their emission-line characteristics been thoroughly discussed. We have obtained spectra for 24 of the 27 galaxies in C97. Spectra for two of the remaining galaxies were obtained by Schneider, Schmidt, & Gunn (1994) and were kindly provided by the authors for inclusion in our analysis. Spectra for the galaxy 1519+5050 (CG 693) have been published elsewhere (Weistrop et al. 1992) and will be included in this discussion.

In § 2 our sample is defined. The observations and data reductions are described in § 3. Techniques for analyzing the data are described in § 4. Descriptions of each galaxy in our sample are given in § 5. The classification of two systems in our sample as closely interacting galaxy pairs is discussed in § 6. Section 7 is a summary of the results and conclusions. Section 8 contains a brief discussion of the context of the results from C97 and this paper.

2. THE GALAXY SAMPLE

Our sample is defined as the galaxies that were known to lie in the Bootes void when the imaging data were acquired in 1993. The galaxies in the sample are listed in Table 1. Since then, additional Bootes void galaxies have been reported by Aldering et al. (1995, identifications not yet published) and Szomoru, van Gorkom, & Gregg (1996, hereafter S96). The 18 galaxies of S96, not included in our sample, were identified in an H I survey of the region. Identification of the H I galaxy 1517+3949 was published earlier by Szomoru et al. (1993). This galaxy is included in our sample.

The sample consists mainly of ELGs for which redshifts were obtained by follow-up observations of galaxies identified in either the *IRAS* Point Source Catalog (1985) or low-dispersion spectroscopic surveys, primarily the Case Low-Dispersion Northern Sky Survey (Sanduleak & Pesch 1987, 1989; Pesch & Sanduleak 1989). Detection of galaxies in such surveys suggests either the presence of nuclear activity or recent star formation. Therefore, selection of a sample of galaxies from these surveys produces a bias toward ELGs. These selection effects must be considered when evaluating the group properties of our sample. Furthermore, follow-up surveys in which some of the void galaxies were identified are not complete, thus our sample does not represent a complete sample.

3. OBSERVATIONS AND REDUCTIONS

Our spectra were obtained with the 40 inch (1 m) telescope at Mount Laguna Observatory, Mount Laguna, CA. The observing log is given in Table 2. Column (1) gives the UT dates on which data were taken. Column (2) denotes whether or not the night was photometric. Column (3) lists the galaxies observed on a given night. Column (4) lists the number of integrations. Column (5) is the total integration time per object in seconds.

The spectra were taken using the CCD grism spectrograph, with a 50 mm focal reducer. In this configuration, the TI CCD with an 800 × 800 pixel format has a wavelength range of approximately 4000–7500 Å, with a scale of 6.7 Å pixel^{-1} and a spectral resolution of approximately 18 Å. The slit width is 4.″5–5″, approximately 3 pixels on the CCD. This wide slit covered approximately 20% to 50% of the surface areas of the void galaxies as resolved on the images of C97. The spatial scale on the CCD is 1.″56 pixel^{-1}.

The calibrations performed include bias, overscan, and flat field corrections. Multiple dome flats taken each night were used to make the flat-field corrections. Wavelength calibration was derived using spectra from helium, neon, and argon calibration lamps. The zero point of the wavelength solution was determined from the positions of seven bright night-sky lines of oxygen, mercury, and sodium. Flux calibration and extinction corrections were derived from observations of standard stars (Barnes & Hayes 1982). The contribution of the night sky was subtracted from the individual spectra, and then these spectra were combined.

TABLE 2
OBSERVING SUMMARY

UT Date (1)	Photometric (2)	Galaxy (3)	Integrations (4)	Total Time (s) (5)
1993 May 25.....	Yes	1407+4840	3	3600
	...	1428+5255	2	2400
	...	1530+4332	3	3600
	...	1517+3956	...	...
	...	...	1	1200
	...	...	2	2400
1993 May 26.....	No	1547+5121	2	2400
	...	1540+5013	2	2400
	...	1519+5050	2	2400
1994 May 13.....	No	1406+4905	3	3600
	...	1413+5056	3	3600
	...	1537+5315	3	3600
	...	...		
1994 May 14.....	Yes	1408+4852	3	3600
	...	1444+4402	3	3600
	...	1510+4727	3	3600
	...	1535+3831	3	3600
	...	1506+5138	3	3600
1994 May 15.....	Yes	1432+5302	3	3600
	...	1446+4457	3	3600
	...	1457+4228	3	3600
	...	1505+3958	3	3600
	...	1458+4944	3	3600
1995 May 21.....	No	1517+3949	3	3600
	...	1503+5428	3	3600
	...	1507+4554	3	3600
1995 May 24.....	No	1510+4727	...	...
	...	...	2	2400
	...	...	2	2400

4. ANALYSIS OF SPECTRA

The results from the analysis of the galaxies in our sample are listed in Table 3. The galaxy designation is listed in column (1). Column (2) gives alternate identifications. Columns (3)–(15) are the fluxes of emission lines normalized to the flux at the reference wavelength, 5500 Å. Normalized fluxes are reported instead of absolute fluxes due to the nonphotometric observing conditions under which some of the data were taken. The fluxes were not normalized to Hβ, as is often done, because Hβ was not present in emission in all galaxies with emission lines. Column (16) shows the equivalent width of the Hα + [N II] complex. These values are negative because they represent emission lines. Equivalent width is defined to be positive for absorption features. Columns (17)–(19) are the equivalent widths of stellar absorption features. The 41–50 continuum color index is reported in column (20). Column (21) lists the mean flux at 5500 Å. The blended lines of Hα (6563 Å) and [N II] (6548 and 6583 Å) were identified in all of the galaxies except 1503+5428, 1535+3831, and 1537+5315, for which the spectra contained no detectable emission features. A reference redshift was determined for each galaxy from the position of the Hα + [N II] complex, and was used to identify other features (both absorption and emission) in the spectrum. Then redshifts were calculated using all of the detected emission and absorption features.

The uncertainties in our flux measurements include contributions from sky noise (which includes readout noise), errors in the placement of the continuum, and Poisson counting statistics for the continuum and the emission line itself. These factors were added in quadrature to arrive at an overall estimate of the uncertainty in the flux of each line. The 1 σ uncertainties are reported in Table 3. We compared the redshifts measured from our spectra with published redshifts. The rms of the differences is 0.0007, indicating good agreement between the redshifts measured from our spectra and those previously published.

To properly carry out the analysis of the spectra, it was necessary to measure the flux in the Hα line separately from the [N II] doublet. In our low-resolution spectra, these lines are severely blended and could not be satisfactorily deblended using the standard algorithms in IRAF. Therefore, an alternate method was developed. At a spectral resolution of 18 Å, only Hα lines with widths greater than 820 km s^{-1} are resolved. Typically, this amount of broadening in the Balmer lines is only observed in Seyfert 1 galaxies. Because only a small fraction of ELGs are Seyfert 1s (Salzer, MacAlpine, & Boroson 1989), it is reasonable to assume that the Hα lines in the majority of our galaxies are unresolved and that the shapes of these lines correspond to the instrumental profile. In addition, if a galaxy had a broadened Hα line, the Hβ line would also be broadened. No broadening beyond the instrumental profile was observed for any of the Hβ lines detected. The [N II] lines in this complex are never broader than the Hα line and, therefore, would also have instrumental profiles. Thus, we were able to reproduce the shape of the Hα + [N II] complex for a given galaxy by blending three template lines with instrumental profiles at positions determined from the redshift. The line templates were modeled from the strong helium line at 7065 Å present in the helium calibration spectra. The ratio of the line intensities in the [N II] doublet is assumed to be $(\lambda 6548/\lambda 6583) = 0.34$. The difference between the

TABLE 3

SUMMARY OF SPECTROSCOPIC DATA FOR THE BOOTES VOID GALAXIES

Galaxy (1)	ID (2)	Hδ (3)	Hγ (4)	[O III] λ4363 (5)	Hβ (6)	[O III] λ4959 (7)	[O III] λ5007 (8)	HeI λ5876 (9)	[O I] λ6300 (10)	[O I] λ6364 (11)
1345+4641		...	...	...	...	...	...	...	...	...
1357+4641		...	...	...	8.40 ± 0.61	12.90 ± 0.61	21.85 ± 0.54	...	...	...
1406+4905	I Zw 81	...	...	...	5.00 ± 0.08	3.25 ± 0.08	7.21 ± 0.08	...	...	...
1407+4840	CG 910	...	...	...	...	...	...	...	...	...
1408+4852	CG 370	...	5.37 ± 0.32	...	14.68 ± 0.21	11.00 ± 0.19	28.03 ± 0.23	5.37 ± 0.18	2.26 ± 0.19	4.54 ± 0.19
1413+5056		...	...	...	...	...	...	...	...	...
1428+5255		...	...	...	...	2.60 ± 0.12	2.99 ± .13	...	...	...
1432+5302	CG 474	6.91 ± 0.32	20.72 ± 0.34	2.13 ± 0.31	52.38 ± 0.31	58.32 ± 0.32	183.24 ± 0.51	8.70 ± 0.20	5.25 ± 0.43	1.72 ± 0.55
1444+4402	CG 538	...	...	...	6.07 ± 0.11	0.74 ± 0.10	1.19 ± 0.09	...	...	...
1446+4457	CG 547	...	2.54 ± 0.15	...	7.52 ± 0.11	5.89 ± 0.11	10.41 ± 0.11	2.17 ± 0.11	1.70 ± 0.22	1.06 ± 0.24
1457+4228	CG 598	...	...	...	9.62 ± 0.12	4.83 ± 0.10	12.06 ± 0.13	...	...	...
1458+4944	CG 922	...	6.87 ± 0.41	...	16.19 ± 0.30	10.15 ± 0.26	26.29 ± 0.31	...	...	...
1503+5428	CG 620	...	...	...	...	...	...	...	...	...
1505+3958	CG 629	...	...	...	5.21 ± 0.19	3.21 ± 0.15	5.73 ± 0.16	...	...	...
1506+5138	Mrk 845	...	...	...	...	4.26 ± 0.11	5.07 ± 0.13	...	...	...
1507+4554	CG 642	35.25 ± 2.62	52.84 ± 2.26	...	118.93 ± 2.17	167.04 ± 2.67	469.78 ± 4.61	22.86 ± 1.07	...	...
1510+4727	CG 657	12.90 ± 0.43	30.88 ± 0.43	...	52.15 ± 0.34	77.80 ± 0.42	226.93 ± 0.64	7.50 ± 0.25	9.78 ± 0.36	7.35 ± 0.32
1517+3949		...	...	...	...	6.09 ± 0.32	6.59 ± 0.34	...	...	...
1517+3956	CG 684	...	6.92 ± 0.30	...	27.22 ± 0.23	19.86 ± 0.20	58.70 ± 0.27	4.03 ± 0.18	4.67 ± 0.18	1.70 ± 0.17
1519+5050	CG 692	...	5.11 ± 0.36	...	20.30 ± 0.25	8.06 ± 0.23	19.21 ± 0.24	...	...	...
1530+4332A ...	Main	...	...	...	8.33 ± 0.19	...	4.83 ± 0.16	...	...	...
1530+4332B....	Companion	...	...	...	10.07 ± 0.30	5.16 ± 0.37	18.51 ± 0.36	...	...	...
1535+3831		...	...	...	...	...	...	...	...	...
1537+5315		...	...	...	...	...	...	...	...	...
1540+5013		...	...	...	...	...	...	...	...	...
1547+5121		...	...	...	5.55 ± 0.37	7.62 ± 0.32	8.76 ± 0.33	...	...	...

TABLE 3—*Continued*

Galaxy (1)	[N II] λ6548 (12)	Hα (13)	[N II] λ6583 (14)	[S II] λλ6717, 6731 (15)	EW(Hα + [N II]) (16)	EW(G band) (17)	EW(Mg *b*) (18)	EW(Na D) (19)	41–50 (20)	*F*(5500 Å) (21)
1345 + 4641	...	42.00 ± 0.78	...	11.10 ± 0.71	−37.01 ± 0.67	...	...	...	...	0.10
1357 + 4641	...	24.02 ± 0.30	...	4.72 ± .025	−44.41 ± 0.56	...	...	...	...	0.10
1406 + 4905	5.01 ± 0.10	23.01 ± 0.10	15.17 ± 0.10	7.77 ± 0.09	−43.85 ± 0.28	2.35 ± 0.17	2.20 ± 0.15	...	0.16 ± 0.08	3.16
1407 + 4840	3.71 ± 0.19	24.07 ± 0.21	11.23 ± 0.20	9.14 ± 0.22	−33.89 ± 0.30	...	2.23 ± 0.25	3.53 ± 0.18	0.64 ± 0.16	0.97
1408 + 4852	...	61.36 ± 0.30	...	17.97 ± 0.21	−74.07 ± 0.48	3.88 ± 0.27	...	...	0.18 ± 0.09	0.59
1413 + 5056	...	12.88 ± 0.31	...	4.64 ± 0.32	−11.75 ± 0.36	4.92 ± 0.33	9.82 ± 0.95	...	0.72 ± 0.20	0.67
1428 + 5255	1.57 ± 0.15	12.46 ± 0.16	4.77 ± 0.15	5.56 ± 0.23	−20.95 ± 0.29	7.20 ± 0.33	3.96 ± 0.28	3.42 ± 0.19	0.76 ± 0.13	2.50
1432 + 5302	4.74 ± 0.24	185.29 ± 0.50	14.35 ± 0.26	36.20 ± 0.0.29	−206.50 ± 0.78	...	...	...	−0.03 ± 0.08	1.02
1444 + 4402	2.86 ± 0.09	31.60 ± 0.11	8.68 ± 0.10	9.75 ± 0.10	−49.91 ± 0.24	2.14 ± 0.15	...	...	0.43 ± 0.06	1.60
1446 + 4457	1.71 ± 0.12	34.96 ± 0.13	5.19 ± 0.12	11.17 ± 0.14	−45.13 ± 0.26	...	0.77 ± 0.11	...	0.28 ± 0.07	0.54
1457 + 4228	4.97 ± 0.13	54.18 ± 0.16	15.07 ± 0.14	15.41 ± 0.16	−78.90 ± 0.34	...	...	...	0.24 ± 0.07	2.31
1458 + 4944	9.00 ± 0.24	47.71 ± 0.30	27.28 ± 0.27	18.42 ± 0.29	−127.40 ± 1.09	1.01 ± 0.17	...	...	0.16 ± 0.09	0.95
1503 + 5428	...	...	...	...	...	...	...	...	0.08 ± 0.56	0.13
1505 + 3958	3.10 ± 0.18	17.58 ± 0.19	9.41 ± 0.19	6.75 ± 0.21	−29.98 ± 0.44	...	5.02 ± 0.37	...	0.34 ± 0.11	1.23
1506 + 5138	1.13 ± 0.13	10.91 ± 0.14	3.43 ± 0.15	...	−16.10 ± 0.32	4.21 ± 0.27	5.93 ± 0.35	...	0.62 ± 0.10	1.03
1507 + 4554	4.10 ± 0.90	308.00 ± 4.40	12.42 ± 1.15	62.83 ± 1.54	−455.00 ± 5.08	...	...	...	−0.12 ± 0.35	1.52
1510 + 4727	21.23 ± 0.23	135.25 ± 0.38	64.35 ± 0.30	26.75 ± 0.25	−406.50 ± 2.20	...	...	...	−0.12 ± 0.17	0.40
1517 + 3949	0.71 ± 0.36	20.22 ± 0.39	2.15 ± 0.37	8.89 ± 0.38	−25.43 ± 0.85	...	...	...	0.39 ± 0.22	0.29
1517 + 3956	8.12 ± 0.19	112.67 ± 0.27	24.60 ± 0.21	35.72 ± 0.24	−154.00 ± 0.55	3.11 ± 0.23	1.82 ± 0.23	...	0.25 ± 0.08	0.92
1519 + 5050	10.08 ± 0.21	50.28 ± .25	30.55 ± 0..23	16.59 ± 0.21	−131.60 ± 0.69	...	...	...	0.14 ± 0.10	1.09
1530 + 4332A ...	5.13 ± 0.22	31.30 ± 0.24	15.55 ± 0.23	10.98 ± 0.25	−51.95 ± 0.59	9.02 ± 0.54	...	...	0.48 ± 0.19	0.77
1530 + 4332B....	2.15 ± 0.77	26.36 ± 0.83	6.52 ± 0.78	8.66 ± 0.83	−50.22 ± 1.16	6.86 ± 0.50	...	...	0.21 ± 0.24	0.45
1535 + 3831	...	...	...	...	...	...	...	...	0.30 ± 0.11	0.92
1537 + 5315	...	...	...	...	...	...	...	...	0.30 ± 0.22	0.87
1540 + 5013	...	27.42 ± 0.23	...	...	−23.85 ± 0.35	2.78 ± 0.26	...	...	0.61 ± 0.14	1.30
1547 + 5121	2.82 ± 0.22	29.26 ± 0.66	8.53 ± 0.35	15.85 ± 0.29	−46.58 ± 0.70	...	2.39 ± 0.40	4.45 ± 0.51	0.28 ± 0.23	0.54

NOTES.—Cols. (17)–(20) are in Å. The flux at 5500 Å in Column (21) is in units of in units of 10^{-15} ergs cm^{-2} s^{-1} Å^{-1}.

continuum-subtracted spectrum of the galaxy and the template spectrum was used to create a residual spectrum. By adjusting the Hα and [N II] template intensities, we minimized the deviations from the mean in the residual spectrum. The combination which produced the minimum deviation in the residual spectrum was chosen as the best fit to the Hα + [N II] complex. The best fits typically had values of the rms that were within $\pm 10\%$ of the rms in the galaxy continuum. The fluxes in the components of the Hα + [N II] complex were then measured from the scaled templates.

Uncertainties in the line fluxes due to deblending were estimated from the range of scale factors that produced residuals less than twice the rms in the continuum. The variation in the template fluxes corresponding to this range of scale factors was defined as the uncertainty in the line flux due to the deblending process. These uncertainties were added in quadrature to the measurement uncertainties described above.

A correction must be made to the measured fluxes of the Balmer emission lines to compensate for hydrogen absorption features in the underlying stellar continuum. This correction is generally made by the addition of a constant based on a uniform estimate of the equivalent widths of the hydrogen absorption features (Kennicutt 1992, hereafter K92; Contini, Davoust, & Considere 1995; Liu & Kennicutt 1995). PTP adopted an equivalent width of 2 Å to correct for the underlying Balmer absorption. Because these 10 galaxies are included in our sample and we wish to compare with PTP, we also adopt a correction of EW = 2 Å.

In the absence of nuclear activity, a galaxy's stellar population governs the shape of the continuum emission. We extracted the mean continuum shapes of the galaxies to examine the flux distribution as a function of wavelength and constrain the stellar populations. None of the galaxy continua have been corrected for reddening; therefore the true continua are probably even bluer than they appear. Continua that increase toward shorter wavelengths indicate either large numbers of O and B stars or blue nonthermal emission due to nuclear activity.

Quantitative measurements of the shapes of the continua were made using the 41–50 continuum color index defined by K92. The 41–50 color index is given by the expression

$$41\text{–}50 \equiv 2.5 \log \left[f_\nu(5000)/f_\nu(4100) \right] , \qquad (1)$$

where f_ν is the rest-frame flux per unit frequency. The 41–50 colors for the galaxies in our sample are listed in Table 3 (col. [20]). For comparison, the 41–50 colors of stars from each spectral type, from the library of stellar spectra compiled by Jacoby, Hunter, & Christian (1984), are given in Table 4. The continuum colors are not corrected for reddening, consistent with K92.

Stellar absorption features, such as Na D lines and Mg *b* and G bands, have been identified in the spectra of many of the galaxies in the sample. These absorption features indicate the presence of a population of late-type stars. The absence of these lines in a continuum with a good signal-to-noise ratio (S/N) implies a stellar population dominated by early-type stars. These absorption features, combined with the 41–50 color index and the continuum shape, are analyzed to constrain the stellar components of the Bootes void galaxies.

We use line-intensity diagnostics to determine whether the ELGs in the void are H II region–like galaxies (H II galaxies) or AGNs. Baldwin, Phillips, & Terlevich (1981) and Veilleux & Osterbrock (1987, hereafter VO87) have shown that ELGs having different sources of photoionizing radiation can be distinguished from one another using diagrams of line-intensity ratios. The line fluxes used in this analysis were corrected for underlying Balmer absorption as described previously. Diagrams of the line diagnostics are presented in Figures 1 and 2. The fluxes were not corrected for reddening, which would move the points slightly farther up and to the right than indicated in these figures. However, ratios between lines of similar wavelength were chosen deliberately to minimize the effects of reddening, as well as errors in flux calibration. In these figures, the solid curve represents the boundary between H II galaxies and AGNs defined by VO87. Typically, H II galaxies lie on the left side of this curve, and the AGNs on the right. A "transition zone" exists around the curve with a width of approximately ± 0.15 on the horizontal axis (VO87). ELGs of both types are found to lie within this transition zone. Classifications of the void galaxies using these diagnostics are discussed in § 5.

TABLE 4
41–50 Comparison Stars

Star (1)	Spectral Type (2)	41–50 (3)
HD 191978.....	O8.5	−0.31
HD 256413.....	B5	0.16
HD 240296.....	A6	0.08
BD + 61 367	F5	0.34
BD + 281885	G5	0.58
HD 21110	K4	1.44
SAO 62808.....	M5	1.61

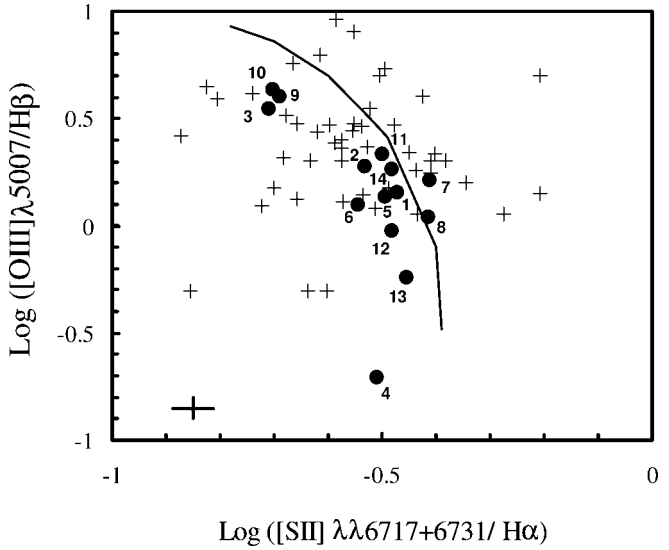

Fig. 1.—Line-intensity diagnostic diagram for flux ratios of [O III] $\lambda 5007/\mathrm{H}\beta$ vs. [S II] $(\lambda 6717+\lambda 6731)/\mathrm{H}\alpha$. The filled circles are the Bootes void galaxies. The crosses are the sample of ELGs from K92. The error bar in the lower left shows the average 2 σ error for the void galaxies. The solid curve is the division between H II galaxies and AGNs defined by VO87. The numbers identify the void galaxies: (1) 1406+4905; (2) 1458+4802; (3) 1432+5302; (4) 1444+4402; (5) 1446+4457; (6) 1457+4228; (7) 1458+4944; (8) 1505+3958; (9) 1507+4554; (10) 1510+4727; (11) 1517+3956; (12) 1519+5050; (13) 1530+4332A; (14) 1530+4332B.

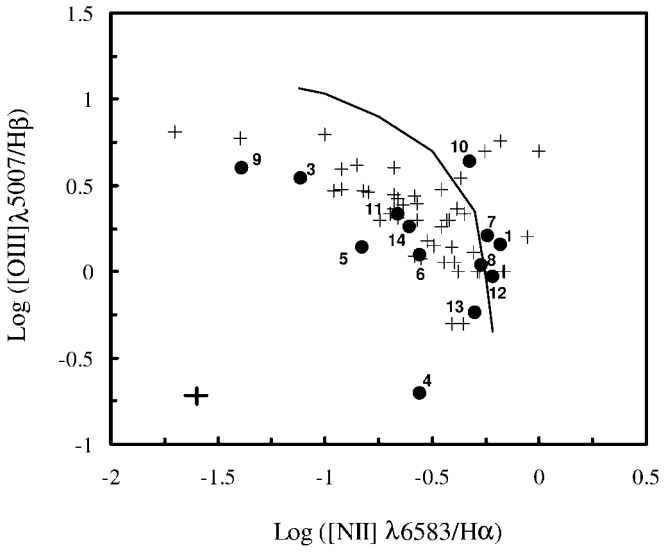

FIG. 2.—Line-intensity diagnostic diagram for flux ratios of [O III] λ5007/Hβ vs. [N II] λ6583/Hα. The filled circles are the Bootes void galaxies. The crosses are the sample of ELGs from K92. The error bar in the lower left shows the average 2 σ error for the void galaxies. The solid curve is the division between H II galaxies and AGNs defined by VO87. The void galaxies are identified using the same numbers as in Fig. 1.

5. DESCRIPTION OF INDIVIDUAL GALAXIES

In this section the individual galaxy spectra are discussed. All of the galaxy spectra are shown in Figures 3*a*–3*z* with fluxes normalized to the continuum flux at 5500 Å. Kennicutt & Kent (1983, hereafter KK83) have shown a correlation between the flux in the Hα + [N II] complex and the star formation rate within a galaxy. They find that among normal galaxies with Hα emission, the EW(Hα + [N II]) $\leq$ 50 Å. The average EW(Hα + [N II]) for their sample is ~19 Å. K92 states that among galaxies with normal star formation rates the EW(Hα + [N II]) $\leq$ 40 Å. These values of EW(Hα + [N II]) are used as references with which to compare the void galaxies to look for enhanced star formation.

1345+4641: The spectrum of this galaxy was provided to us by D. Schneider, M. Schmidt, & J. E. Gunn (1997, private communication). Hα and a weak [S II] feature are the only emission lines detected (Fig. 3*a*). A weak feature is present near the expected position of Hβ; however, the redshift calculated from this line does not agree with the other two emission lines and it is not considered a detection. For this galaxy, EW(Hα) = 37 Å, which is within the range of galaxies with normal star formation rates (K92).

The continuum of this galaxy rises sharply toward shorter wavelengths between 4500 and 5500 Å and is mostly flat between 5500 and 7500 Å, consistent with the color $V-R = 0.30 \pm 0.12$ (C97). This continuum shape indicates the presence of blue stars and recent star formation.

1357+4641: D. Schneider et al. (1997, private communication) provided the spectrum of this galaxy. The EW(Hα + [N II]) = 44 Å, which is near the upper limit for galaxies with normal star formation rates (K92). The characteristics of its spectrum suggest that 1357+4641 is an H II galaxy (Fig. 3*b*). The continuum increases at wavelengths shorter than 5300 Å indicating the presence of blue stars, which is compatible with the Hα and [O III] emission. These data suggest that the galaxy has experienced a recent star formation episode. It is also known to be an X-ray source (Kim et. al. 2001).

1406+4905 (I Zw 81): We detect several emission features, as well as stellar absorption features suggesting the presence of late-type stars (Fig. 3*c*). A significant population of cooler stars is consistent with the continuum shape of this galaxy, which increases toward longer wavelengths, strongly from 4000 to 5000 Å and gradually at wavelengths longer than 5000 Å. The continuum shape is also consistent with the moderately red broadband colors (C97).

Based on line-intensity diagnostics, VO87 classify this galaxy as a "narrow-line AGN" and PTP find it to be a LINER. The interpretation of our spectra is consistent with these findings, but somewhat more ambiguous. Deblending of the Hα + [N II] complex reveals the presence of relatively strong [N II] $\lambda\lambda$6548, 6583 lines, with a [N II]/Hα ratio of 0.87. The enhanced [N II] emission is consistent with this galaxy being an AGN. Line-intensity ratios, including λ6583, place this galaxy in the AGN region of Figure 2 near the transition zone. In Figure 1, however, this galaxy falls in the region of the H II galaxies. Also, any blue nonthermal emission from an AGN is not strongly contributing to the continuum of this galaxy. Because our slit is ~50% wider than that used by PTP, our spectra include more emission from outside the nucleus, possibly diluting the nuclear spectrum.

1407+4840 (CG 910): The emission features in this galaxy are Hα + [N II] and [S II] $\lambda\lambda$6717, 6731 (Fig. 3*d*). No other emission features are detected. Stellar absorption bands of Na D, Mg *b*, and the G band are also present. The EW(Hα + [N II]) = 34 Å, within the range of galaxies with normal star formation rates (K92). Sage et al. (1997) find an unusual distribution of CO emission, suggesting the possibility of tidal interaction. However, imaging of this galaxy shows no evidence of such an interaction (C97).

The continuum of 1407+4840 increases gradually toward long wavelengths. The 41–50 color index is 0.64, red compared with the sample average (consistent with C97). These data suggest that the continuum of this galaxy is dominated by mid- to late-type stars, consistent with the presence of the stellar absorption features.

1408+4852 (CG 370): This galaxy is a disturbed system with a tidal tail (C97). Spectra show several prominent emission features, including He I λ5876 (Fig. 3*e*). The λ5876 line is produced in non-AGN galaxies by O-type stars (Anderson 1972), pre–main-sequence stars (Catala et al. 1993; Ulrich & Wood 1981), and/or a warm diffuse ionized medium (Martin & Kennicutt 1997), all of which indicate recent star formation.

Deblending of the Hα line was attempted, but the [N II] emission derived was negligible. This is consistent with the relatively weak λ6583 emission observed by PTP. Despite the apparent low flux of the [N II] emission, the EW(Hα + [N II]), 74 Å, suggests a high rate of star formation (K92).

The line-intensity indicates that 1408+4852 is an H II galaxy and not an AGN, in agreement with the interpretation of PTP.

The continuum of this galaxy increases toward short wavelengths and has a blue 41–50 color index of 0.18. These data are consistent with its blue broadband colors (C97). 1408+4852 appears to have a large population of blue stars which were probably formed in a recent episode of star formation, possibly triggered by tidal interaction.

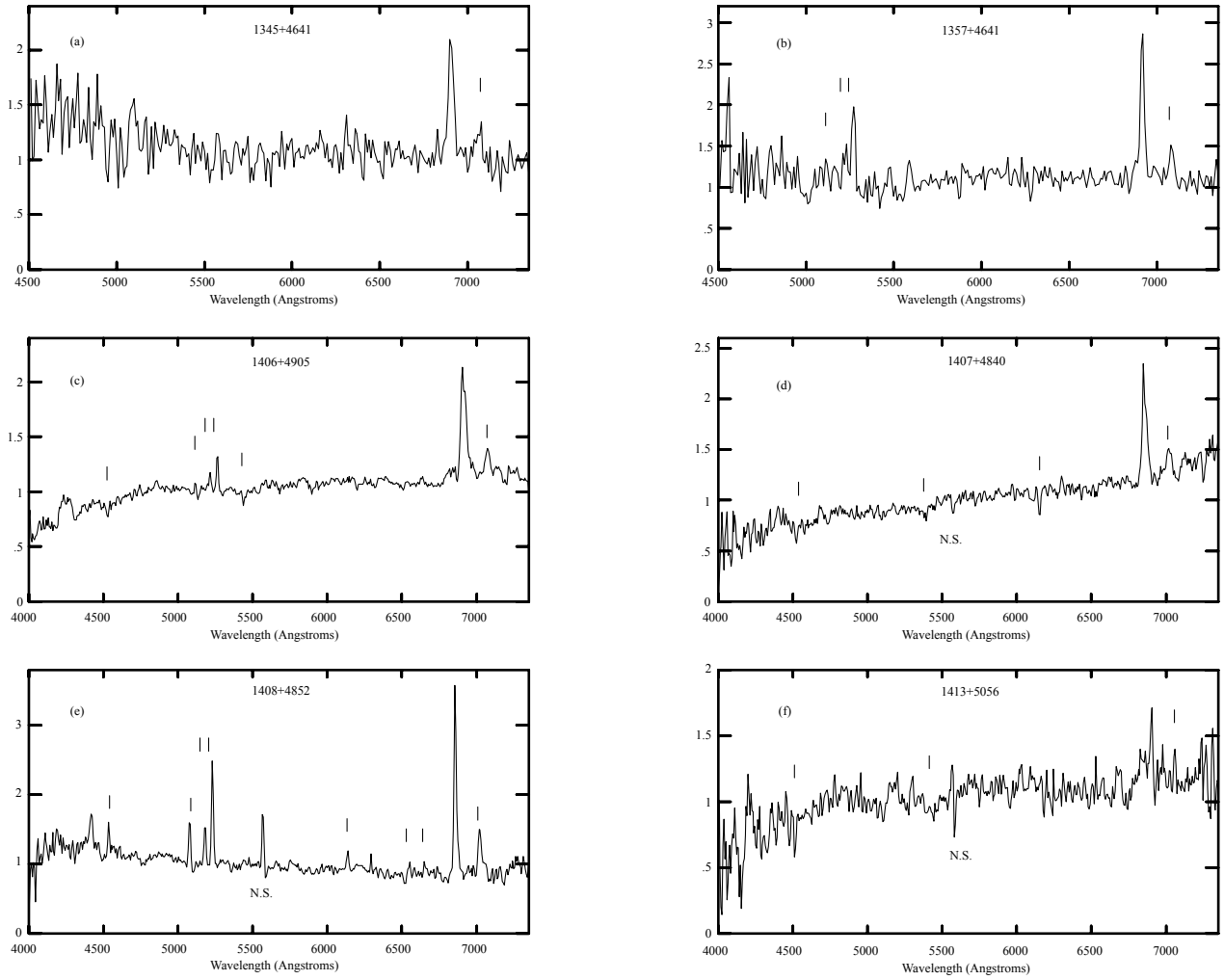

FIG. 3.—Spectra for our sample of Bootes void galaxies. The fluxes are normalized to the continuum fluxes at 5500 Å, which are listed in column (21) of Table 3. The Hα + [N II] emission feature is prominent in the majority of spectra between 6500 and 7000 Å and is not marked. Other spectral features listed in Table 3 are marked. Features labeled " N.S." are the result of incomplete night-sky subtraction. The spectra of 1345+4641 and 1357+4641 were kindly provided to us by D. Schneider et al. (1997, private communication).

1413+5056: This galaxy has a double nucleus (C97). The only prominent emission feature is Hα, with EW(Hα) = 12 Å (Fig. 3*f*). The Hβ line is present in absorption, along with the Mg *b* and G-band absorption features. The continuum shows an increase toward long wavelengths consistent with the broadband colors (C97). The color index is 41–50 = 0.72, red compared with the average of our sample. These data suggest that 1413+5056 has an mature stellar population with a modest rate of star formation compared with other galaxies with Hα emission. This appears to be inconsistent with the galaxy's unusual morphology. However, Kennicutt et al. (1987) have noted that starburst episodes triggered by tidal interactions are not long lived. This galaxy might be a post-starburst system, possibly the result of a merger, although higher S/N spectra would be needed to confirm this.

1428+5255: This galaxy has been identified as a Seyfert 2 by Moran, Halpern, & Helfand (1994) and as an X-ray source by Kim et. al. (2001). The Hα + [N II] emission feature is present with EW(Hα + [N II]) = 21 Å (Fig. 3*g*). The Na D, Mg *b*, and G-band absorption features are also detected. Hβ may be present in absorption.

The continuum increases strongly with wavelength, having a red 41–50 color index of 0.76, consistent with its red broadband colors (C97). This galaxy appears to have a stellar population dominated by late-type stars. No contribution to the blue continuum due to nonthermal emission from the AGN is detected.

The spectrum of 1428+5255 published by Moran et al. (1994) was taken on a 2 m–class telescope. Their spectrum is very similar to ours, having similar emission-line intensities with the same absorption features and general continuum shape. The principal difference is they detect a weak Hβ emission feature, which we do not. It is possible that we included more of the stellar component of the galaxy in our spectrum, resulting in greater Balmer absorption, which might have masked any Hβ emission.

1432+5302 (CG 474): This galaxy has many prominent emission lines (Fig. 3*h*). The He I λ5876 is present indicating recent star formation. The EW(Hα + [N II]) = 207 Å, which is very large even compared with a sample of ultraluminous *IRAS* mergers (Liu & Kennicutt 1995). Using the ratio of intensities of the [O III] lines (λ4959 + λ5007)/λ4363, and assuming an electron density of Ne = 10^3, we estimate a

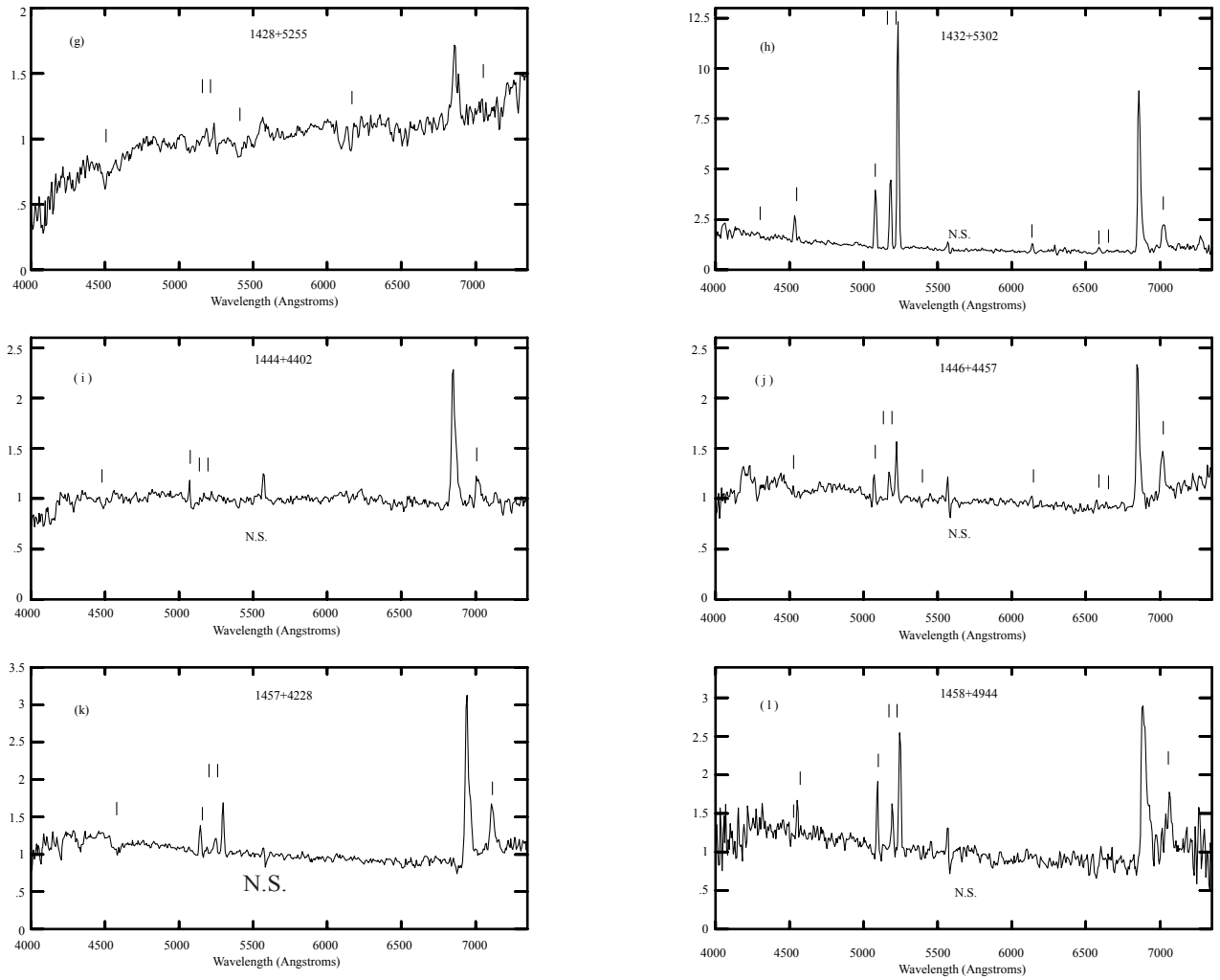

FIG. 3.—*Continued*

nebular temperature of 1.3×10^4 K, within the typical range for H II regions.

1432+5302 has $\lambda 5007/\mathrm{H}\beta > 3$ and [N II]/H$\alpha \approx 0.15$; the latter is more than a factor of 3 lower than the mean value in galaxies with Hα emission (K92). Although galaxies with [O III] $\lambda 5007/\mathrm{Hb} > 3$ are typically high-ionization AGNs (VO87), the most energetic H II galaxies also satisfy this criterion, but typically have relatively weak [N II] emission. Allen et al. (1991) have called these H II galaxies extreme starburst (ESB) galaxies, and they are thought to be the youngest examples of violent star formation episodes.

The line ratios and large EW(Hα + [N II]) suggest 1432+5302 is an ESB galaxy. The data of PTP are in good agreement with ours, suggesting that most of the emission arises in the nucleus. This assertion is consistent with Hα imaging (Weistrop et al. 1995, hereafter W95), which shows strong emission concentrated in the nucleus.

The continuum of 1432+5302 increases at wavelengths shorter than ~5200 Å, consistent with the blue broadband colors measured by C97. There is also an increase in the continuum toward the long-wavelength end of the spectrum (>6800 Å). This feature suggests the presence of late-type stars, possibly young, red supergiants that form approximately 10^7 yr after a starburst episode. The models of Leitherer et al. (1999) show that these red supergiants produce such a feature in the spectral energy distribution of an instantaneous starburst after about 9 million yr. The same feature is not observed in models of continuous star formation, suggesting that 1432+5302 is experiencing a sudden starburst event. The 41–50 color index is −0.03, which is in agreement with the very blue broadband colors of this galaxy (C97). These colors, combined with the strength of the emission features, are indicative of a strong nuclear starburst.

1444+4402 (CG 538): Prominent emission features are detected from this galaxy (Fig. 3*i*), including Hα with an EW(Hα + [N II]) = 50 Å, near the upper limit for galaxies with normal star formations rates (K92). The G-band absorption feature is also present.

The continuum is relatively flat between 5000 and 7000 Å, and the 41–50 color index is 0.43. These data are in agreement with the moderate broadband colors measured by C97. The decrease in the continuum short of 4500 Å and the presence of G-band absorption are consistent with a population of late-type stars.

1446+4457 (CG 547): This is a disk galaxy with the nucleus located off center (C97), which has been found to be an X-ray source (Kim et. al. 2001). The He I $\lambda 5876$

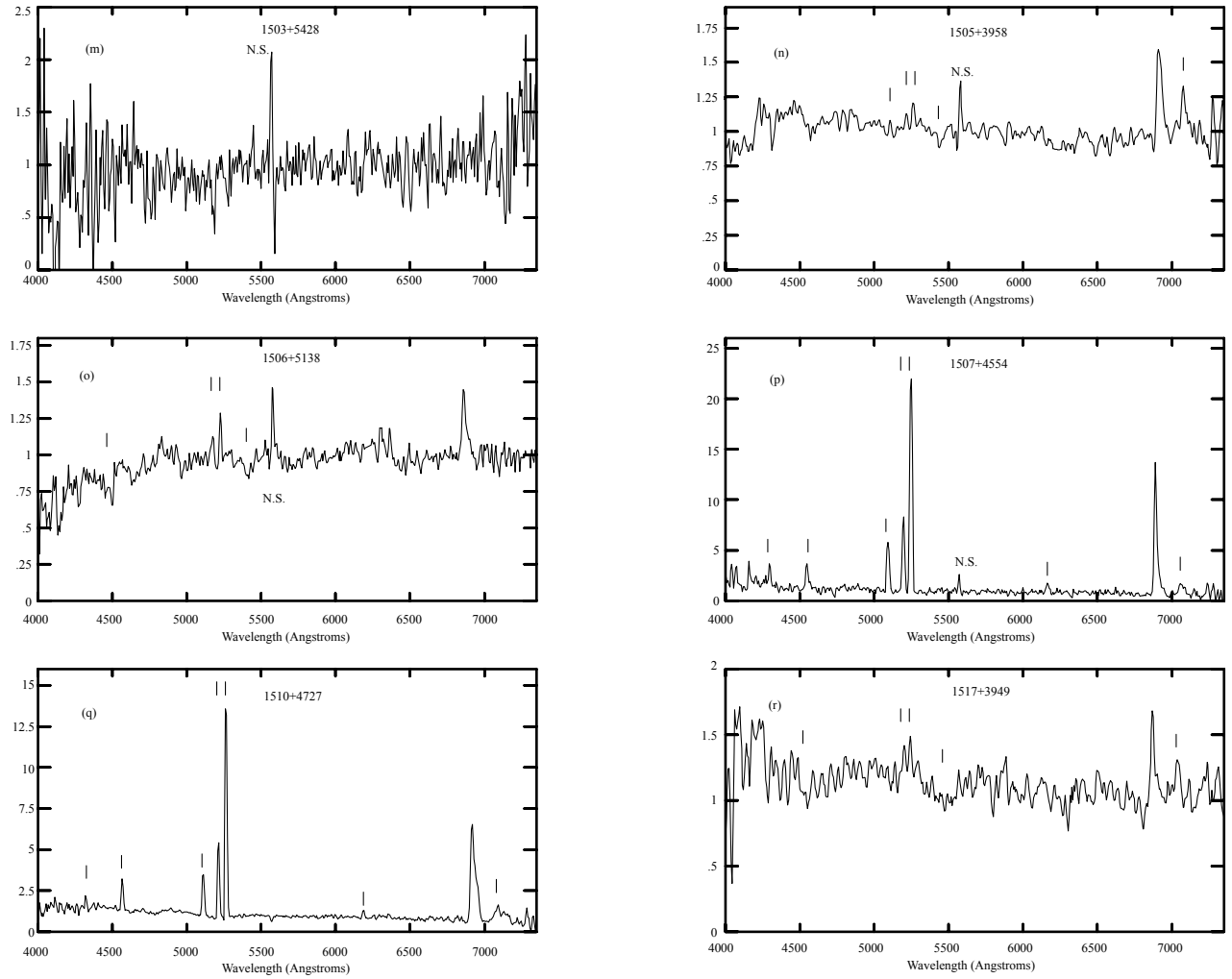

FIG. 3.—*Continued*

line indicates the presence of young stars (Fig. 3*j*). The EW(Hα + [N II]) = 45 Å, which is near the upper limit for galaxies with normal star formation rates (K92).

The line-intensity ratios place 1446+4457 in the transition zone in Figure 1, but clearly in the region of H II galaxies in Figure 2. We classify it as an H II galaxy, in agreement with PTP. However, our λ5007/Hβ ratio is approximately 30% greater than that measured by PTP. The S/N in our spectra is low, and the flux measured in the lines is sensitive to the placement of the continuum level. Setting the continuum is further complicated by the stellar absorption at Hβ. The discrepancy in line ratios is probably due to difficulties in determining the continuum level of the Hβ line.

The continuum of this galaxy increases toward short wavelengths between 4000 and 6000 Å, indicating the presence of a significant fraction of blue stars. The continuum also rises at wavelengths greater than 7000 Å. Given that the Mg *b* absorption line is present, this continuum feature suggests a population of late-type stars. Given the presence of significant emission lines, this rise in the red continuum is likely due to young, red supergiants, as discussed above, and implies a recent star formation episode in this galaxy. The 41–50 color index for this galaxy is 0.28. These data are in agreement with the moderately blue broadband colors measured by C97.

1457+4228 (CG 598): Many of the characteristics of this galaxy resemble those of 1446+4457. The morphologies of the galaxies appear remarkably similar, each having a bright nucleus located off center in a surrounding disk (C97). A dip in the continuum near 4550 Å is the G-band absorption feature, possibly blended with Hγ in absorption (Fig. 3*k*). The EW(Hα + [N II]) = 79 Å, which implies a high rate of star formation compared with normal galaxies with Hα emission (K92).

Based on line-intensity ratios (Figs. 1 and 2), we classify this galaxy as an H II galaxy, in agreement with PTP. However, as with 1446+4457, our λ5007/Hβ ratio is greater than that measured by PTP, probably for the same reason. The shape of the continuum of 1457+4228 is also similar to 1446+4457, suggesting a large number of blue stars and a measurable contribution from cool stars that are likely to be young, red supergiants. The 41–50 color index is 0.24, which is in agreement with the moderately blue broadband colors measured by C97.

1458+4944 (CG 922): The spectrum of this galaxy is shown in Figure 3*l*. The Hα + [N II] feature is very strong relative to the continuum, with EW(Hα + [N II]) = 127 Å.

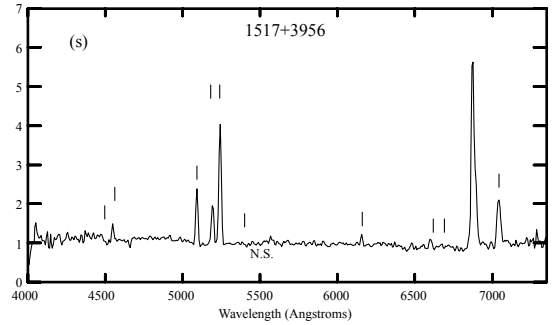

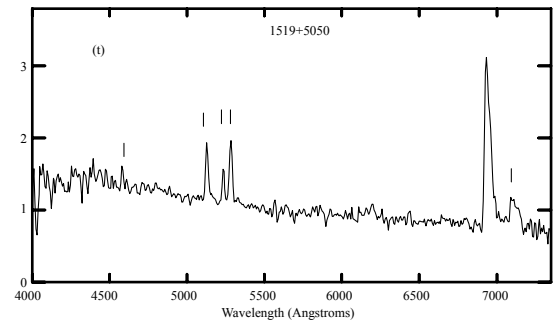

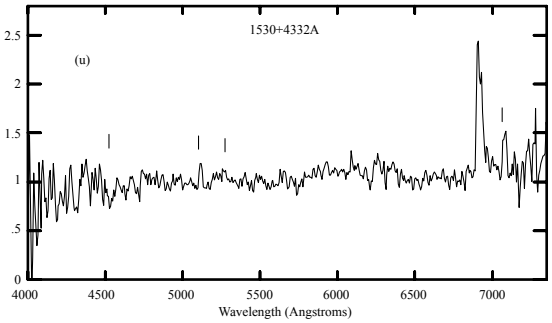

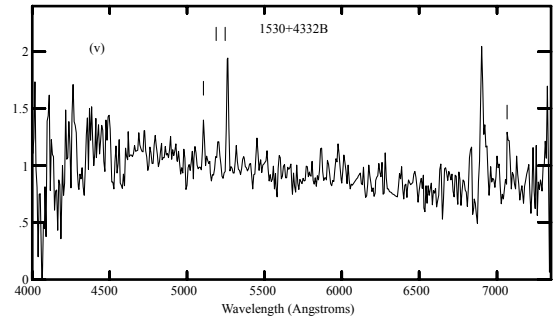

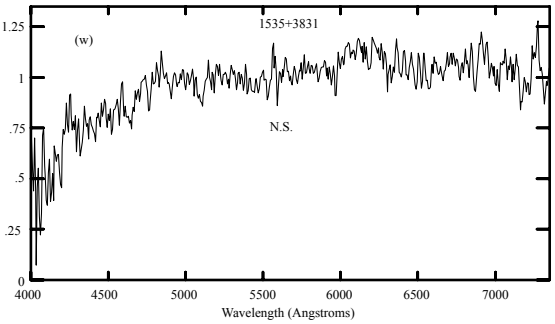

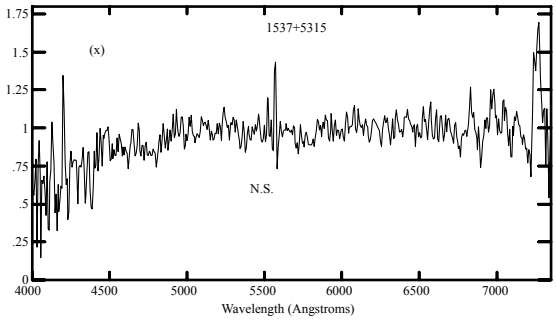

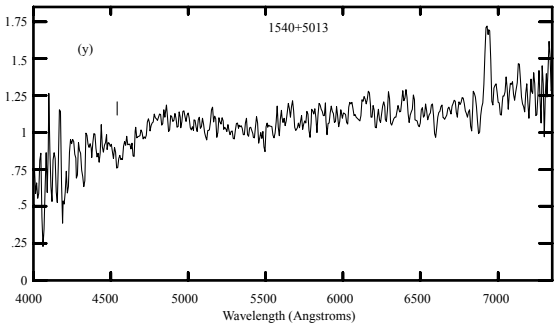

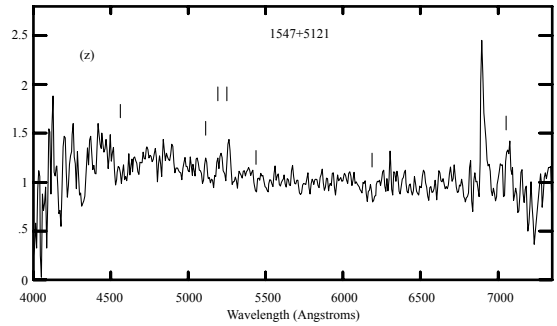

FIG. 3.—*Continued*

The emission from forbidden lines is strong, and line-intensity diagnostics place this galaxy within the AGN region in both Figures 1 and 2. In Figure 2, however, the galaxy falls close to the dividing line between H II galaxies and AGNs.

The continuum increases sharply toward shorter wavelengths, and the 41–50 color index is 0.16. These properties are consistent with the blue broadband colors reported by C97. An increase in flux at wavelengths longer than 6500 Å and the presence of G-band absorption suggest a contribution to the continuum from late-type stars. This galaxy was unresolved in broadband imaging, yet it is relatively bright ($Mv = -19.84 \pm 0.07$) compared with the other unresolved galaxies in the Bootes void sample (C97). This morphology is consistent with nuclear emission. 1458+4944 is also a source of significant X-ray emission (Kim et. al. 2001), consistent with nuclear activity.

Considering all of these data, we classify 1458+4944 as an AGN. Because it has $\lambda5007/\mathrm{H}\beta < 3$, it is most likely a LINER (VO87). This galaxy has not been previously classified as an AGN.

1503+5428 (CG 620): We detect no emission or absorption lines from this galaxy (Fig. 3*m*). The mean flux from the continuum is 1.33×10^{-16} ergs cm^{-2} s^{-1} Å^{-1}.The weakest lines detected in other galaxies in our sample have EW > 1 Å. If we consider EW = 1 Å as the detection limit, then the Hα + [N II] flux from 1503+5428 must be less than 1.33×10^{-16} ergs cm^{-2} s^{-1} Å^{-1}. Spectra of this galaxy were not taken under photometric conditions, so the true flux limit is uncertain. Spectra from which the redshift was originally measured have not been published. The continuum increases toward longer wavelengths, which is consistent with the red broadband colors measured by C97.

1505+3958 (CG 629): This galaxy has significant Hα + [N II] emission (Fig. 3*n*) with EW(Hα + [N II]) = 30 Å, within the range of galaxies with normal star formation rates (K92). The analysis of the line-intensity diagnostics for this galaxy is not straightforward. In Figure 1 1505+3905 falls in the region occupied by AGNs. In contrast, PTP measure line intensities that place it in the transition zone very near the dividing line between AGNs and H II galaxies. Most notably, the $\lambda5007/\mathrm{H}\beta$ ratio from our spectra is a factor of 3 greater than that reported by PTP. In Figure 2 1505+3958 falls along the dividing line between AGNs and H II galaxies. The galaxy's location on this diagram is also significantly different than is suggested by the line intensities of PTP, which place the galaxy well within the area occupied by H II galaxies.

The S/N in both sets of measurements is low, and the discrepancy between our data and PTP may be the result of measurement uncertainty. However, if this galaxy does harbor an AGN, the differences in the line intensities could be caused by variability of the emission lines. Peterson, Crenshaw, & Meyers (1985) report changes in the $\lambda5007/\mathrm{H}\beta$ ratio from AGNs with magnitudes comparable to the difference between our data and PTP and over timescales shorter than the difference in our observing dates.

The difference in the line ratios could also arise from differences in the width and alignment of the observing slits. If the emission emanates from a weak nuclear AGN and surrounding H II regions, then small changes in slit alignment could affect the observed line ratios. Considering all the data, the evidence is not strong enough to classify this galaxy as an AGN; therefore, it is categorized as an H II galaxy.

The continuum gradually increases toward shorter wavelengths between 4500 and 6500 Å. The 41–50 color index is 0.34, the same as that of an F star. The shape of the continuum appears inconsistent with the color indices given by C97 ($B-V = 0.79 \pm 0.07$; $V-R = 0.30 \pm 0.04$). Because the broadband colors are integrated over the entire galaxy and the spectra are dominated by emission near the nucleus, the color indices may be redder than the spectra due to population gradients across the galactic disk.

1506+5138 (Mrk 845): Osterbrock & Dahari (1983) have classified 1506+5138 as a Seyfert 1. Kim et. al. (2001) report significant X-ray emission with rapid and large-amplitude flux variations, an effect they suggest may be indicative of narrow-line Seyfert 1s. In our spectra, the flux from the stellar continuum dominates the nuclear emission lines (Fig. 3*o*). The only prominent emission feature is the Hα + [N II] complex. The 41–50 color index for this galaxy is 0.62, which is consistent with the red broadband colors measured by C97. We do not detect a strong contribution to the continuum due to blue nonthermal emission from the AGN. This galaxy does have a very bright, circular nucleus (C97) consistent with its classification as an AGN.

1507+4554 (CG 642): This galaxy has very strong emission lines (Fig. 3*p*), including the He I line $\lambda5876$, indicating the presence of young stars. The Hα + [N II] complex is remarkably strong with respect to the continuum, having an EW(Hα + [N II]) = 455 Å.

Line-intensity diagnostics places this galaxy in the regions in Figures 1 and 2 occupied by highly energetic H II galaxies with $\lambda5007/\mathrm{H}\beta > 3$. This result agrees with the data of PTP. Because this galaxy is not an AGN, the substantial EW(Hα + [N II]) implies an enormous rate of star formation (K92). For these reasons, we classify 1507+4554 as an ESB galaxy.

The strengths of the emission lines compared with the continuum provide the most likely explanation of the unusual broadband colors measured by C97 ($B-V = 0.92 \pm 0.09$; $V-I = -0.02 \pm 0.14$). These colors are consistent with additional flux in the *V* filter, centered at approximately 5300 Å, due to strong emission lines. The redshifted Hβ and [O III] $\lambda\lambda4959$, 5007 lines lie near the center of this bandpass, and they have a combined EW equal to 246 Å.

The continuum flux increases at wavelengths shorter than 5000 Å. The 41–50 color index is quite blue at −0.12, very nearly that of a B star (−0.16), suggesting a large number of young stars and providing further evidence that the broadband colors do not represent continuum emission but are strongly influenced by emission lines. These data are further evidence for recent and strong star formation activity within this galaxy.

1510+4727 (CG 657): This system is a closely interacting galaxy pair (§ 6). The spectrum is shown in Figure 3*q* and includes the He I $\lambda5876$ line indicating recent star formation. The EW(Hα + [N II]) = 407 Å, which is extremely large compared with normal galaxies with Hα emission (K92).

Analysis of the line-intensity ratios for 1510+4727 yields curious results. The [S II] lines are relatively weak with respect to Hα. However, because of a very large $\lambda5007/\mathrm{H}\beta$ ratio, this system falls in the region of Figure 1 near the ESB galaxies. In Figure 2, significant [N II] emission relative to Hα places this system among the AGNs. The line-intensities reported by PTP make this difference in classification even more pronounced and would place this system farther to the

left in Figure 1 and farther to the right in Figure 2. However, neither of these sets of observations are in agreement with Weistrop & Downes (1988), who classify this galaxy as an H II galaxy based on its location in Figure 2.

Finally, because of the mechanism that produces [O I] emission in nebulae, Baldwin et al. (1981) and VO87 find that the ratios of $\lambda5007/H\beta$ compared with [O I] $\lambda6300/H\alpha$ are the most sensitive discriminator between AGNs and H II galaxies. The [O I] emission arises primarily in a region of partially ionized hydrogen that is much larger in nebulae ionized by the power-law spectra of AGNs than in nebulae ionized by O and B stars. A sufficient flux is measured in the [O I] $\lambda6300$ line to classify this galaxy as an AGN. However, the S/N of the $\lambda6300$ line is weak, making accurate measurement difficult.

The continuum emission from 1510+4727 increases strongly toward shorter wavelengths over the entire spectrum, which is consistent with its blue broadband colors (C97). The 41–50 color index is also quite blue at -0.12, very nearly that of a B star (-0.16). The blue continuum shape of this system certainly suggests a large fraction of blue stars. Blue nonthermal emission from an AGN may also be contributing to the continuum.

PTP classify 1510+4727 as an H II galaxy, but they were unaware of this system being an interacting pair. Whether the data showed evidence of nuclear activity could depend strongly on the slit alignment relative to the two galaxies, possibly accounting for this difference in spectra. Tidal interaction may have stimulated nuclear activity that is responsible for the [O I] lines and the excess [N II] emission (Lin, Pringle, & Rees 1988). Higher resolution spectra of each half of this system are needed to determine whether or not it contains an AGN.

1517+3949: This galaxy was first identified in an H I survey. Its published redshift was determined from the 21 cm line (Szomoru et al. 1993). We have identified optical emission lines in the spectrum at the redshift of the H I data (Fig. 3*r*). The $H\alpha + [N\ II]$ complex is detected with an EW($H\alpha + [N\ II]$) = 25 Å. Stellar absorption features are also detected, indicating the presence of late-type stars.

The continuum gradually increases toward short wavelengths with a moderately blue 41–50 color index of 0.39, consistent with the broadband colors (C97). These data indicate a significant number of hot stars combined with the population of cool stars suggested by the stellar absorption bands. Szomoru et al. (1993) report that this galaxy is associated with the active star-forming system 1517+3956 and has an "irregular surface density distribution" in H I possibly caused by an interaction with the distant (~670 kpc) companion. The EW($H\alpha + [N\ II]$) does not suggest recent widespread star formation due to a tidal interaction.

1517+3956 (CG 684): This system is a closely interacting galaxy pair (§ 6). The spectrum shown is of the southern half of the system (i.e., 3*s*). The spectrum of the northern half is similar. He I $\lambda5876$ emission is detected suggesting the presence of young stars. The EW($H\alpha + [N\ II]$) = 154 Å, indicating strong star formation. Based on line-intensity ratios (Figs. 1 and 2), we classify this galaxy as an H II galaxy, in agreement with PTP. The presence of an OH megamaser within this system suggests violent star formation activity (Bottinelli et al. 1989; Baan, Salzer, & Lewinter 1998).

The spectrum indicates the presence of O and B stars combined with a population of cool stars, indicated by the presence of G band and Mg *b* absorption. The 41–50 color index for 1517+3956 is 0.25, consistent with its blue broadband colors (C97). This galaxy is undergoing active star formation triggered by tidal interaction.

1519+5050 (CG 692/693): This is a pair of interacting spiral galaxies. The larger (northwest) galaxy, CG 692, has a single, extended spiral arm distorted by the tidal interaction (Weistrop et al. 1992; W95). CG 692 is classified as an H II galaxy with widespread star formation, and CG 693 as a Seyfert 1 (Weistrop et al. 1992). Kim et. al. (2001) report strong X-ray emission primarily from CG 693, consistent with this classification. Our spectra of CG 692 include a section of the single spiral arm and a region of strong $H\alpha$ emission, along with the nucleus (Fig. 3*t*). No new spectra of CG 693 were taken.

We find CG 692 to have a 41–50 color index of 0.14, EW($H\alpha + [N\ II]$) = 132 Å, and line-intensity ratios that confirm classification as an H II galaxy. All of these data suggest recent star formation activity and a large fraction of young blue stars, supporting the interpretations Weistrop et al. (1992), W95, and C97.

1530+4332: This is a galaxy pair separated by ~22 kpc (20″). The main galaxy, 1530+4332A, is located west of its smaller companion, 1530+4332B (W95). The $H\alpha + [N\ II]$ feature in 1530+4332A has EW($H\alpha + [N\ II]$) = 52 Å (Fig. 3*u*), near the upper limit for galaxies with normal star formation rates (K92). Line-intensity diagnostics leads to the classification of this galaxy as an H II galaxy (Figs. 1 and 2).

The continuum increases toward longer wavelengths over the observed wavelength range. The 41–50 color index is 0.48, which is redder than our sample average, and the broadband colors for this galaxy are also moderately red. These colors and the presence of G-band absorption indicate a population of late-type stars.

The $H\alpha + [N\ II]$ complex in 1530+4332B has EW($H\alpha + [N\ II]$) = 50 Å (Fig. 3*v*), near the upper limit for galaxies with normal star formations rates (K92). We classify this galaxy as an H II galaxy based on line-intensity diagnostics.

1530+4332B has a moderately blue 41–50 color index of 0.21, consistent with its broadband colors (C97). The continuum features indicate the presence of many hot O and B stars combined with a population of cool stars indicated by the presence of G-band absorption.

1535+3831: We detect no emission lines from this galaxy. Dey et al. (1990) report a radial velocity of 15,398 ± 41 km s^{-1} for this object measured from emission lines visible in a 20 minute integration with the 3 m telescope at Lick Observatory. However, emission-line fluxes are not published. In our spectra, the mean flux from the continuum near the expected position of $H\alpha$ is 9.77×10^{-16} ergs cm^{-2} s^{-1} Å^{-1} (Fig. 3*w*). Employing the approximate detection limit discussed above, the $H\alpha + [N\ II]$ flux must be less than 9.77×10^{-16} ergs cm^{-2} s^{-1} Å^{-1}. $H\beta$ may be present in absorption. The continuum increases toward longer wavelengths over the entire wavelength range. This continuum shape agrees well with the red broadband colors of this galaxy (C97).

1537+5315: This galaxy has a single elongated spiral arm or tidal tail (C97). We detect no emission lines, consistent with the results of W95. The radial velocity, 15,776 ± 23 km s^{-1}, was measured by Dey et al. (1990). We estimate the upper limit of the $H\alpha + [N\ II]$ flux to be less than 8.72×10^{-16} ergs cm^{-2} s^{-1} Å^{-1} (Fig. 3*x*). Spectra of this galaxy were not taken under photometric conditions. The

continuum increases toward longer wavelengths, consistent with its red broadband colors (C97). The absence of measurable emission from this disturbed galaxy may indicate that it has evolved into a post-starburst phase (Kennicutt et al. 1987).

1540+5013: The only emission line present is Hα with EW(Hα) = 24 Å (Fig. 3*y*), in the range for galaxies with normal star formations rates (K92). G-band absorption is detected and Hβ may be present in absorption. The continuum increases toward longer wavelengths. The continuum shape agrees well with the red broadband colors (C97).

1547+5121: This is an edge-on galaxy with an asymmetric disk. The EW(Hα + [N II]) is 47 Å (Fig. 3*z*), near the upper limit for galaxies with normal star formations rates (K92). The emission-line properties indicate that this is an H II galaxy. Beyond 6800 Å, the spectrum increases gradually toward longer wavelengths. This galaxy has a moderately blue 41–50 color index of 0.28, consistent with its broadband colors (C97). The spectrum indicates the presence of O and B stars combined with a cool stellar population.

6. INTERACTING GALAXY PAIRS

The galaxy systems 1510+4727 and 1517+3956 have asymmetric or disturbed morphologies (Moody et al. 1987; W95; C97). Both systems have a northern and southern bright nucleus, separated by approximately 4″, suggesting that they may be interacting pairs. Individual spectra of the northern and southern nuclei were taken. The redshifts were determined from the wavelengths of all the unblended emission lines (Figs. 4 and 5). The redshift for the northern bright nucleus in 1517+3956 is $z = 0.0464 \pm 0.0007$, for the southern nucleus $z = 0.0479 \pm 0.0005$. Moody et al. (1987) published a velocity for this system corresponding to $z = 0.0475$, which lies between our two values. The velocity difference measured from the unblended emission lines is $\Delta v = 449 \pm 50$ km s^{-1}, in agreement with the velocity difference between two CO emission features detected in radio observations, $\Delta v = 497 \pm 24$ km s^{-1} (Sage et al. 1997).

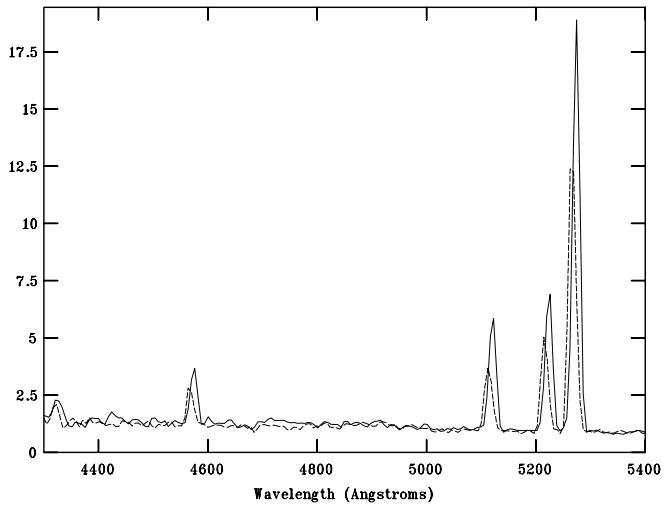

FIG. 4.—Spectra of the two nuclei of 1510+4727 (CG 657) normalized to the flux at 5500 Å. The solid line is the southern nucleus and the dashed line is the northern nucleus. These spectra indicate a velocity difference of 388 ± 21 km s^{-1}.

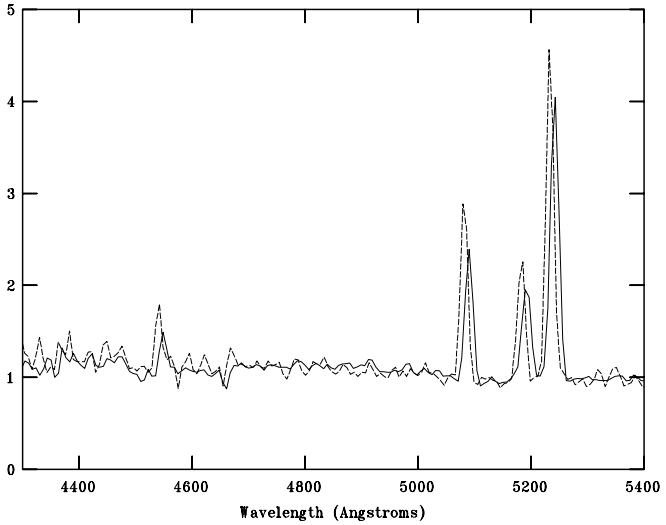

FIG. 5.—Spectra of the two nuclei of 1517+3956 (CG 684) normalized to the flux at 5500 Å. The solid line is the southern nucleus and the dashed line is the northern nucleus. These spectra indicate a velocity difference of 400 ± 66 km s^{-1}.

Fourier cross-correlation analysis was used to determine the shift in wavelength between the spectra from the two bright regions in this system (Tonry & Davis 1979). Cross-correlation analysis makes use of all of the features of the spectrum, emission lines, stellar absorption features, and structure in the continuum. The velocity difference between the two bright nuclei is calculated to be 400 ± 66 km s^{-1}. The error is estimated by propagating the uncertainty due to noise in the cross-correlation function through the calculation of the centroid for the cross-correlation peak. This value is in good agreement with velocity difference calculated from the unblended emission lines and the CO data. We conclude that the velocity difference in 1517+3956 is real with $\Delta v = 400 \pm 66$ km s^{-1}.

For 1510+4727, we measure redshifts of $z = 0.0543 \pm 0.0004$ for the southern nucleus and $z = 0.0529 \pm 0.0006$ for northern nucleus. Moody et al. (1987) published a velocity corresponding to $z = 0.0535$, which lies between our two redshifts. Using the unblended emission lines, the velocity difference between the nuclei is 420 ± 25 km s^{-1}. A Fourier cross-correlation analysis of the spectra from each nucleus of 1510+4727 yields a velocity difference of 388 ± 21 km s^{-1}. This value agrees within the errors with that derived from the emission lines.

Because of the unusual morphologies, strong emission lines, and velocity differences of these systems, we conclude that 1510+4727 and 1517+3956 are closely interacting galaxy pairs. This result was previously suggested for 1517+3956 by Weistrop (1994) and for 1510+4727 by C97. We have since obtained images of 1517+3956 with the *Hubble Space Telescope* that confirm this system is an interacting pair (Cruzen et al. 2002).

7. RESULTS

We report spectroscopy for 26 galaxies in the Bootes void. Emission lines and absorption features were identified in 23 of the 26 galaxies, including 1517+3949, in which optical

emission lines were identified for the first time. No emission or absorption features were detected in the spectra of 1503+5428, 1535+3831, and 1537+5315. For the remaining 23 galaxies, redshifts were calculated using all of the available lines. Nearly all of the measured redshifts agree with published redshifts within the uncertainty of the measurement.

For galaxies with Hα + [N II] emission, the EW(Hα + [N II]) are compared with samples of field and cluster galaxies having Hα emission (KK83 and K92). Of the 23 void galaxies with Hα + [N II] lines, 11 have EW(Hα + [N II]) $\geq$ 50 Å and are experiencing powerful starburst episodes. Six of these galaxies have EW(Hα + [N II]) $\geq$ 88 Å, the mean value for a sample of ultraluminous *IRAS* mergers (Liu et al. 1995). These large values for EW(Hα + [N II]) indicate strong star formation activity among many of the void galaxies.

We use line-intensity diagnostics to classify 16 of the void galaxies as H II galaxies or AGNs. Fourteen galaxies are H II galaxies. Two of these systems, 1432+5302 and 1507+4554, are classified as ESBs. The presence of ESB galaxies indicates that intense star formation is taking place in the current epoch in some void galaxies. However, the presence of stellar populations containing metals in many of the galaxies indicates that the void galaxies are not experiencing their first generation of star formation. Seven of the H II galaxies have morphologies suggesting that current star formation may be triggered by tidal interaction (C97).

Five of the galaxies have emission lines in their spectra, but not the lines necessary for classification as H II galaxies or AGNs. The classification for these galaxies remains unknown.

The line-intensity diagnostics identifies 1458+4944 as an AGN for the first time. 1406+4905 was previously classified as a LINER by PTP. Our analysis of this galaxy is consistent with this result, although somewhat uncertain. Including these two galaxies, at least five AGNs are known within the Bootes void. The line ratios in 1510+4727 suggest that it might contain an AGN. However, this result is ambiguous. Approximately 20% of the ELGs in the void are AGNs, which is large compared with ~11% of field ELGs (Salzer et al. 1989). The small numbers involved make the significance of this difference uncertain. Because of the large slit through which our spectra were obtained, stellar emission from the galaxy bulge and/or disk may overwhelm nuclear emission lines. Therefore, the number of AGNs in the void may be underestimated.

A summary of the classifications of the void galaxies is given in Table 5. For comparison, the relative line intensities of a sample of ELGs from K92 (his Table 1) are plotted with the void galaxies in Figures 1 and 2. In both figures, the void galaxies appear to follow the distribution of ELGs closely. In Figure 1, however, the void galaxies seem to be somewhat more tightly clustered around the transition zone. This distribution might indicate slightly greater flux in [S II] $\lambda\lambda$6717, 6731 among the void sample than in the field galaxies. This enhanced [S II] emission was also noted by PTP.

Analysis of the 41–50 color indices of this sample indicates good agreement with the photometric results from C97. Nine galaxies have continua that increase strongly toward short wavelengths at wavelengths less than 5500 Å. Nearly all of these galaxies have strong emission lines, and only three have stellar absorption features in their spectra. These data imply a significant number of O and B stars within these galaxies. These hot stars dominate the galaxy continuum.

TABLE 5

CLASSIFICATIONS FOR THE BOOTES VOID GALAXIES

Galaxy (1)	Type (2)	Comments (3)
1345+4641	...	...
1357+4641	H II	...
1406+4905	AGN	LINER
1407+4840	...	...
1408+4852	H II	...
1413+5056	...	...
1428+5255	AGN	Seyfert 2
1432+5302	ESB	...
1444+4402	H II	...
1446+4457	H II	...
1457+4228	H II	...
1458+4944	AGN	LINER
1503+5428	...	No lines observed
1505+3958	H II	...
1506+5138	AGN	Seyfert 1
1507+4554	ESB	...
1510+4727	H II	Interaction
1517+3949	...	...
1517+3956	H II	Interaction
1519+5050	H II	(CG 692) interaction with CG 693
1519+5050*	AGN	(CG 693) Seyfert 1
1530+4332A ...	H II	(Main) interaction
1530+4332B....	H II	(Companion)
1535+3831	...	No lines observed
1537+5315	...	No lines observed
1540+5013	...	...
1547+5121	H II	...

Fifteen of the galaxies have continua that increase toward longer wavelength, either at wavelengths greater than 6500 Å or over the entire wavelength range. These data imply a population of cool stars, either an underlying population of late-type dwarf stars or a population of young, red supergiants, presumably originating in the star formation event that produced the O and B stars. The galaxies with continua that increase to longer wavelengths typically have metallic absorption features in their spectra, confirming the presence of significant cool stellar populations.

Cohen (1976) has shown a strong correlation between the strength of Balmer emission and galaxy color. KK83 and K92 have verified the correlation between emission-line EW and broadband colors, and continuum colors, respectively. To determine whether our galaxies satisfy this relation, the 41–50 color index is plotted against the EW(Hα + [N II]) in Figure 6 for the void galaxies and the emission-line sample of K92. In this figure the void galaxies fall neatly onto the sequence defined by the majority of the ELGs. Thus, the standard correlation between Balmer emission and continuum color is also seen in the void galaxies, again indicating that they are similar to field ELGs.

Two closely interacting galaxy pairs are identified for the first time. Analysis of spectra from the irregular galaxy systems 1510+4727 and 1517+3956 reveal that each is an interacting galaxy pair. For 1510+4727, the pair have a velocity difference of $\Delta v = 388 \pm 21$ km s^{-1}, according to Fourier cross-correlation analysis. Applying this technique to 1517+3956 yields a velocity difference of $\Delta v = 400 \pm 66$ km s^{-1}. With the addition of 1510+4727 and 1517+3956, at

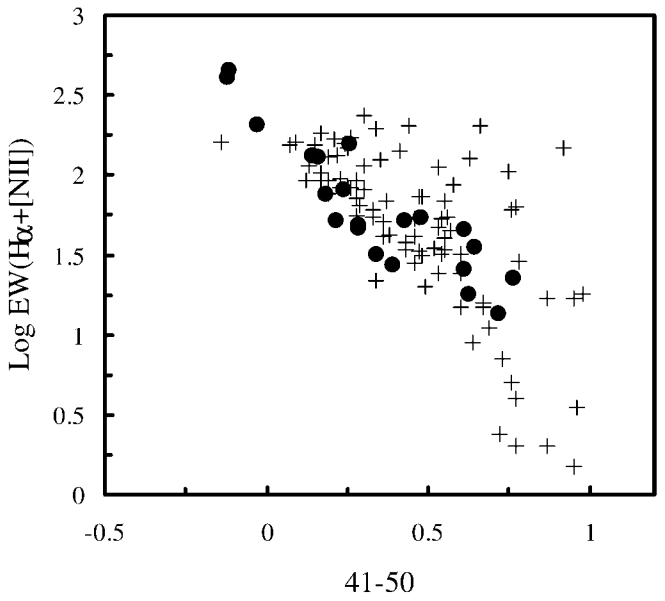

FIG. 6.—Equivalent width of the Hα + [N II] complex vs. the 41–50 continuum color index for the 21 void galaxies that had measurable Hα + [N II] emission and continuum below 4500 Å. The crosses are the sample of ELGs from K92.

least four interacting galaxy pairs are known within the Bootes void (Table 5). The other two pairs are 1519+5050 and 1530+4332. Three of the galaxy pairs are strongly interacting or possibly merging. This number suggests a greater frequency of interacting galaxies in the void than the 8% reported for field ELGs by Salzer et al. (1989), although this conclusion is uncertain due to the small numbers. However, this result agrees with the conclusion of Weistrop et al. (1992) that conditions for producing galaxy interactions are independent of galaxy density, provided that all regions within the void are uniformly underdense. Grogin & Geller (2000) report that 15% of galaxy systems in their lowest-density void sample are pairs, consistent with the 4/25 paired systems in our sample.

8. DISCUSSION

The primary goal of the study of galaxies in low-density environments is to define the void population and to determine how the characteristics of this population constrain models of galaxy formation and evolution and the large-scale distribution of mass in the universe. Because of selection effects in this sample of Bootes void galaxies, the properties of the sample cannot be generalized to define a representative void population. However, these galaxies are an important segment of the population in the Bootes void. The existence of bright, active, star-forming and tidally interacting galaxies in voids constrains models of galaxy evolution in low-density environments.

If global underdensity were the primary factor in controlling the evolution of galaxies in voids, then void populations might well be predominantly faint, unevolved systems. For instance, the models of Hoffman, Silk, & Wyse (1992) suggest that giant, low surface brightness galaxies should inhabit voids. Lacey et al. (1993) state that their models predict no luminous galaxies forming in voids because of a lack of tidal interactions needed to trigger star formation. These conclusions are inconsistent with the observational results reported here and elsewhere (e.g., W95; C97; Popescu, Hopp, & Rosa 1999; Vennik et al. 2000), which describe a void population of active ELGs very similar to those in the field. Therefore, considering the implications of previous observational work with the results from our survey, we conclude that the overall morphological characteristics and internal processes of our sample are not greatly influenced by their global environment. These results agree with those of Grogin & Geller (1999, 2000), who conclude that the local environment plays the dominant role in morphology and the star formation history of ELGs in voids.

By examining the spatial distribution of the *IRAS* galaxies in the Bootes void, Weistrop (1994) identified a vertical "slab" 10 Mpc wide that contained approximately half of the galaxies. This structure is also present in the distribution of our entire sample, and the galaxy density in it is comparable to the density outside the void (Weistrop 1994). Interestingly, this slab contains all four of the galaxy pairs in our sample and nine of 13 galaxies with the highest degree of perturbation (PC $\geq$ 3, C97). This result is consistent with previous suggestions that spatial correlations exist among void galaxies (S96). In an investigation of ELGs in nearby voids, Popescu, Hopp, & Elsässer (1997) report a tendency for clustering among void galaxies and identify a filamentary structure in one void that they term "the arch." Models by van de Weygaert & van Kampen (1993) and Dubinski et al. (1993) predict nonuniform filamentary distributions of matter to evolve within voids.

It is possible that the evolution of galaxies in voids is strongly tied to mass filaments within the voids. The bright, active or star-forming galaxies in voids may have evolved along filaments that provide environments where the local mass density is similar to that in the field. It is possible that these bright ELGs still do not represent the galaxy population in the lowest density environments.

This research was supported in part by NASA through the Nevada Space Grant Consortium and by the Theodore Dunham, Jr., grant from the Fund for Astrophysical Research. The observations for this project were made at the Mount Laguna Observatory, operated jointly by San Diego State University and the University of Illinois. We are grateful to D. Schneider, M. Schmidt, and J. Gunn for kindly providing their spectra of 1345+4641 and 1357+4641. It is also a pleasure to thank L. Spight, D. P. Smith, G. Rhee, and S. Lepp for their numerous suggestions, support, and encouragement. A special thanks to C. Nelson for many important conversations concerning the analysis of these data and to John Kilburg for all the systems support.

REFERENCES

Aldering, G., Bothun, G. D., Kirshner, R. P., & Marzke, R. 1995, BAAS, 26, 1408
Allen, D. A., Norris, R. P., Meadows, V. S., & Roche, P. F. 1991, MNRAS, 248, 528
Anderson, C. M. 1972, ApJ, 177, L121
Baan, W. A., Salzer, J. J., & Lewinter, R. D. 1998, ApJ, 509, 633
Baldwin, J. A., Phillips, M. M., & Terlevich, R. 1981, PASP, 93, 5
Barnes, J., & Hayes, D. 1982, KPNO IRS Standard Star Manual (Tucson: NOAO)
Bottinelli, L., Gouguenheim, L., Le Squeren, A. M., Dennefeld, M., Martin, J. M., & Paturel, G. 1989, IAUC 4928
Catala, C., Bohm, T., Donati, J.-F., & Semel, M. 1993, A&A, 278, 187

Cohen, J. G. 1976, ApJ, 203, 587
Contini, T., Davoust, E., & Considere, S. 1995, A&A, 303, 440
Cruzen, S., Wehr, T., Weistrop, D., Nelson, C., & Angione, R. 2002, in preparation
Cruzen, S., Weistrop, D., & Hoopes, C. 1997, AJ, 113, 1983 (C97)
da Costa, L. N., Freudling, W., Wegner, G., Giovanelli, R., Haynes, M. P., & Salzer, J. J. 1996, ApJ, 468, L5
da Costa, L. N., et al. 1994, ApJ, 424, L1
de Lapparent, V., Geller, M. J., & Huchra, J. P. 1986, ApJ, 302, L1
Dey, A., Strauss, M., & Huchra, J. 1990, AJ, 99, 463
Dressler, A. 1980, ApJ, 236, 351
Dubinski, J., da Costa, A., Goldwirth, D. S., Lecar, M., & Piran, T. 1993, ApJ, 410, 458
El-Ad, H., Piran, T. 2000, MNRAS, 313, 553
Giovanelli, R., Haynes, M. P., & Chincarini, G. L. 1986, ApJ, 300, 77
Grogin, N., & Geller, M. 1999, AJ, 118, 2561
———. 2000, AJ, 119, 32
Hoffman, Y., Silk, J., & Wyse, R. F. G. 1992, ApJ, 388, L13
IRAS Point Source Catalog. 1985, Joint *IRAS* Science Working Group (Washington: GPO)
Jacoby, G. H., Hunter, D. A., & Christian, C. A. 1984, ApJS, 56, 257
Kennicutt, R. C. 1992, ApJ, 388, 310 (K92)
Kennicutt, R. C., & Kent, S. M. 1983, AJ, 88, 1094 (KK83)
Kennicutt, R. C., Roettiger, K. A., Keel, W. C., van der Hulst, J. M., & Hummel, E. 1987, AJ, 93, 1011
Kim, C., Boller, T., Ghosh, K., Swartz, A., & Ramsey, B. 2001, ApJ, 546, L91
Kirshner, R. P., Oemler, A., Schechter, P. L., & Shectman, S. A. 1981, ApJ, 248, L57
———. 1987, ApJ, 314, 493
Lacey, C., Guiderdoni, B., Rocca-Volmerange, B., & Silk, J. 1993, ApJ, 402, 15
Leitherer, C., et al. 1999, ApJS, 123, 3
Lin, D. N. C., Pringle, J. E., & Rees, M. J. 1988, ApJ, 328, 103
Lindner, U., Einasto, J., Einasto, M., Freudling, W., Fricke, K., & Tago, E. 1995, A&A, 301, 329
Liu, C. T., & Kennicutt, R. C. 1995, ApJ, 450, 547
Martin, C. A., & Kennicutt, R. C., Jr. 1997, ApJ, 483, 698
Moody, J. W., Kirshner, R. P., MacAlpine, G. M., & Gregory, S. A. 1987, ApJ, 314, L33
Moran, E. C., Halpern, J. P., & Helfand, D. 1994, ApJ, 433, L65
Müller, V., Arbabi-Bidgoli, S., Einasto, J., & Tucker, D. 2000, MNRAS, 318, 280
Osterbrock, D. E., & Dahari, O. 1983, ApJ, 273, 478
Peimbert, M., & Torres-Peimbert, S. 1992, A&A, 253, 349 (PTP)
Pesch, P., & Sanduleak, N. 1989, ApJS, 70, 163
Peterson, B. M., Crenshaw, D. M., & Meyers, K. A. 1985, ApJ, 298, 283
Popescu, C. C., Hopp, U., & Elsässer, H. 1997, A&A, 325, 881
Popescu, C. C., Hopp, U., & Rosa, M. R. 1999, A&A, 350, 414
Postman, M., & Geller, M. J. 1984, ApJ, 281, 95
Sage, L. Weistrop, D., Cruzen, S., & Kömpe, C. 1997, AJ, 114, 1753
Salzer, J. J., MacAlpine, G. M., & Boroson, T. A. 1989, ApJS, 70, 479
Sanduleak, N., & Pesch, P. 1987, ApJS, 63, 809
———. 1989, ApJS, 70, 173
Sargent, W. L. W. 1970, ApJ, 160, 405
Schneider, D., Schmidt, M., & Gunn, J. E. 1994, AJ, 107, 1245
Strauss, M. A., & Huchra, J. 1988, AJ, 95, 1602
Szomoru, A., van Gorkom, J. H. & Gregg, M. 1996, AJ, 111, 2141 (S96)
Szomoru, A., van Gorkom, J. H., Gregg, M., & de Jong, R. S. 1993, AJ, 105, 464
Tifft, W. G., Kirshner, R. P., Gregory, S. A., & Moody, J. W. 1986, ApJ, 310, 75
Tonry, J., & Davis, M. 1979, AJ, 84, 1511
Ulrich, R. K., & Wood, B. C. 1981, ApJ, 244, 147
van de Weygaert, R. & van Kampen, E. 1993, MNRAS, 263, 481
Veilleux, S., & Osterbrock, D. E. 1987, ApJS, 63, 295 (VO87)
Vennik, J., Hopp, U., & Popescu, C. C. 2000, A&AS, 142, 399
Vogeley, M. S., Geller, M. J., & Huchra, J. P. 1991, ApJ, 382, 44
Weistrop, D. 1989, AJ, 97, 357
———. 1994, in Violent Star Formation from 30 Doradus to QSOs, ed. G. Tenorio-Tagle (Cambridge: Cambridge Univ. Press), 100
Weistrop, D., & Downes, R. A. 1988, ApJ, 331, 172
Weistrop, D., Hintzen, P. A. M., Kennicutt, Jr., R. C., Liu, C. Lowenthal, J., Cheng, K.-P., Oliverson, R., & Woodgate, B. 1992, ApJ, 396, L23
Weistrop, D., Hintzen, P. A. M., Liu, C. Lowenthal, J., Cheng, K.-P., Oliverson, R., Brown, L., & Woodgate, B. 1995, AJ, 109, 981 (W95)